

Topological Resonances in Scattering on Networks (Graphs)

Sven Gnutzmann¹, Holger Schanz^{2,3} and Uzy Smilansky^{4,5}

¹*School of Mathematical Sciences, University of Nottingham, Nottingham NG7 2RD, UK*

²*Institute for Mechanical Engineering, Hochschule Magdeburg-Stendal, 39114 Magdeburg, Germany*

³*Max-Planck-Institute for Physics of Complex Systems, D-01187 Dresden, Germany*

⁴*School of Mathematics, University of Cardiff, Cardiff CF24 4AG, UK*

⁵*Department of Physics of Complex Systems, The Weizmann Institute of Science, Rehovot, Israel*

We report on a hitherto unnoticed type of resonances occurring in scattering from networks (quantum graphs) which are due to the complex connectivity of the graph - its topology. We consider generic open graphs and show that any cycle leads to narrow resonances which do not fit in any of the prominent paradigms for narrow resonances (classical barriers, localization due to disorder, chaotic scattering). We call these resonances ‘topological’ to emphasize their origin in the non-trivial connectivity. Topological resonances have a clear and unique signature which is apparent in the statistics of the resonance parameters (such as e.g., the width, the delay time or the wavefunction intensity in the graph). We discuss this phenomenon by providing analytical arguments supported by numerical simulation, and identify the features of the above distributions which depend on genuine topological quantities such as the length of the shortest cycle (girth). These signatures cannot be explained using any of the other paradigms for narrow resonances. Finally, we propose an experimental setting where the topological resonances could be demonstrated, and study the stability of the relevant distribution functions to moderate dissipation.

Narrow resonances are abundant in a large variety of physical systems, and their immense importance as indicators of long lived states led to an intensive study of their properties and origin. The weak effective coupling to the continuum which underlies their appearance can arise in various circumstances. Common mechanisms are the existence of potential or dynamical barriers such as weakly transmitting optical mirrors in optical Fabry-Perot resonators, dynamical tunneling in systems with a mixed phase space [1, 2] or scarring of quantum states by unstable trapped orbits [3]. Anderson localization in disordered systems [4, 5] induces narrow resonances not because of any barriers but because of destructive interference between multiply scattered waves with random phases while a classical particle diffuses unhindered through the system. Here, the resonance parameters depend on the particular realization of the disorder and must be studied with statistical methods. Statistical methods are also necessary for studying resonances which characterize chaotic scattering [6–11], where fluctuations in the wave functions may lead to approximate bound states with very low amplitude at the interface between the interior of the system and the continuum. This inhibits the transition to the exterior, resulting in a long living state.

Wave propagation on bounded networks (graphs) displays many features which are typical to quantum chaotic systems [12, 13]. When the networks are connected to external leads, the resulting scattering parameters fluctuate, much in the same way as expected from the analysis of chaotic wave-scattering in open Hamiltonian systems [9, 10, 14, 15]. However, in addition to resonances from random-like interfering waves, the non-trivial connectivity is also responsible for the formation of another type of narrow resonances – the subject of the present note. We will show that these resonances exist in a large class of

scattering graphs if the graph contains a cycle. We thus call them ‘topological resonances’. They have properties which clearly distinguish them from other mechanisms leading to narrow resonances: their mark on the distributions of the resonance parameters cannot be explained by any of the other paradigms.

The rest of this letter is organized as follows. The topological resonances signature will first be illustrated with some numerical simulations. The underlying theoretical framework, will then be reviewed, and used to derive the observed resonance distributions in simple cases. Finally, a possible experimental setup is proposed where topological resonances could be observed.

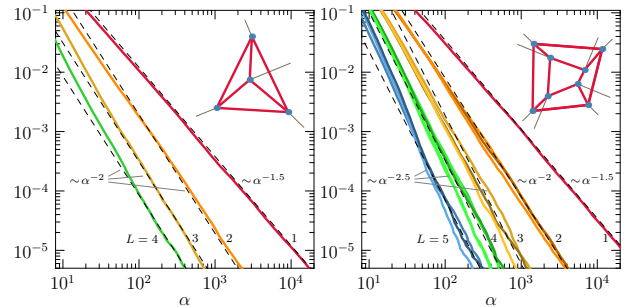


FIG. 1. (Color online) Tails of the integrated distribution $I(\alpha)$ for the mean intensity α . Insets show the underlying graphs. Full lines represent numerical results where $L = 1, \dots, 5$ is the number of attached lead. Note that the data for $L = 2, 3, 4, 5$ for the cube consists of more than one line – these correspond to non-equivalent ways to attach L leads. The dashed lines are power-law tails $\sim \alpha^{-\mu}$ with indicated exponents.

Numerical illustrations: The insets of Fig. 1 show two different networks: a fully connected graph with 4 vertices (tetrahedron) on the left and a graph with 8 vertices

(cube) on the right. The interior of the graph consists of finite bonds between vertex pairs (red lines). Infinite leads (gray lines) are attached to some vertices. Scalar waves propagate freely on the bonds and leads, and at the vertices they are reflected or transmitted without losses. Thus, one has a scattering system, which is described by an $L \times L$ scattering matrix $S(k)$.

Solving the scattering problem numerically with an incoming wave of unit flux and wave number k , we compute the mean intensity $\alpha(k)$ of the wave function on the internal edges (see (4) for an explicit definition). The resulting distributions

$$P(\alpha) = \lim_{K \rightarrow \infty} \frac{1}{K} \int^K \delta(\alpha - \alpha(k)) dk, \quad (1)$$

or rather, their cumulative form $I(\alpha) = \int_\alpha^\infty P(\alpha') d\alpha'$, display extremal power-law distributions shown in Fig. 1, for various L values. The simulation summarized in Fig. 1 and further numerical results for other graphs suggest $I(\alpha) \sim \alpha^{-\mu}$ for large α with

$$\mu = \begin{cases} \frac{L+2}{2} & \text{for } L \leq C - 1 \\ \frac{C+1}{2} & \text{for } L \geq C - 1 \end{cases} \quad (2)$$

where C is the number of bonds on the shortest cycle (girth). The tetrahedron girth is $C = 3$. Thus, one expects the exponent to be $\mu_L = 1.5$ for $L = 1$ and $\mu_L = 2$ for $L \geq 2$. On the other hand, for the cube with $C = 4$ one expects $\mu_1 = 1.5$, $\mu_2 = 2$, and $\mu_L = 2.5$ for $L \geq 2$. This is indeed borne out by the simulations. The appearance of the girth suggests a topological origin.

The result (2) cannot be explained by the other paradigms for narrow resonances. Indeed barriers such as almost perfect mirrors in a Fabry-Perot interferometer lead to a cut-off for the intensity. Scattering from a disordered system gives rise to a power law with a fixed exponent $\mu_{\text{loc}} = 1$ which is independent of the number of channels [4, 5]. Random-matrix models for chaotic scattering predict a power law with an exponent $\mu_{\text{RMT}} = \frac{L+2}{2}$ [6–8] which is only consistent with (2) if $L \leq C - 1$.

We shall now summarize the graph theoretical setting (including the definition of the class of graphs) where topological resonances will be rigorously defined, and equation (2) will be derived.

Quantum Graphs and topological resonances: A scattering graph $G = \{\mathcal{V}, \mathcal{E}\}$ consists of a set of vertices \mathcal{V} and a set of edges $\mathcal{E} = \mathcal{B} \cup \mathcal{L}$ where \mathcal{B} is the set of bonds connecting pairs of vertices and \mathcal{L} the set of infinite leads. The graphs considered here are all of finite cardinality. We will assume that the graph is connected, has no loops (each bond connects two different vertices) and each vertex i has degree (the number of attached edges) $d_i \geq 2$. Thus, graphs with dangling bonds corresponding to vertices with $d = 1$ are excluded. Multiple connections between two vertices are allowed. Each bond $b \in \mathcal{B}$ has a finite length $\ell_b \in (0, \infty)$ and a coordinate $x_b \in [0, \ell_b]$ such that $x_b = 0$ and $x_b = \ell_b$ correspond to the two end

vertices. The leads $l \in \mathcal{L}$ are of infinite length. The coordinate $x_l \in [0, \infty)$ is defined such that $x_l = 0$ is the position of the end vertex.

The complex valued wave function on the graph is written as $\Psi = \{\psi_b(x_b)\}_{b \in \mathcal{B}} \cup \{\psi_l(x_l)\}_{l \in \mathcal{L}} \equiv \{\psi_e(x_e)\}_{e \in \mathcal{E}}$. On each edge the wave function satisfies the Helmholtz (or stationary free Schrödinger) equation $\frac{d^2 \psi_e}{dx_e^2} + k^2 \psi_e = 0$ where $k > 0$ is the wave number. At the vertices the wave function is continuous and $\sum_{e=1}^d \frac{d\psi_e}{dx_e}(0) = 0$, where the sum extends over all edges which emanate from the vertex. These Neumann or Kirchhoff matching conditions are a standard choice from a wider range of admissible boundary conditions [16]. At a given wave number the wave function on any edge has the form

$$\psi_e(x_e) = a_{(e,+)} e^{ikx_e} + a_{(e,-)} e^{-ikx_e} \quad (3)$$

where $a_{(e,-)}$ and $a_{(e,+)}$ are the amplitudes of the two counter-propagating waves on the edge. The mean intensity $\alpha(k)$ on the graph is defined by

$$\alpha(k) = \frac{1}{|\mathcal{B}|} \sum_{b \in \mathcal{B}; \sigma = \pm} |a_{b,\sigma}|^2. \quad (4)$$

If the bond lengths are rationally independent then the spectrum of the quantum graph is purely continuous with generalised eigenstates which are bounded everywhere but are not normalizable. To each value of $k > 0$ one can associate a unitary scattering matrix $S(k)$ [14] that relates the outgoing coefficients on the leads to the incoming ones. Resonances are identified as poles of the scattering matrix when k is in the upper complex k -plane. The (positive) imaginary part of the wave number at a resonance gives the decay rate (width). If the bond lengths are changed continuously so do the positions of the poles of $S(k)$. When bond lengths become rationally dependent some poles may move to the real axis indicating the appearance of a normalizable bound state embedded in the continuum (see [17–19]).

We can now *define* a topological resonance as a pole of the scattering matrix that can be moved to the real line to form a bound state by changing some bond lengths continuously while the graph connectivity and matching conditions remain unchanged.

The main statement of this letter is that for rationally independent bond lengths a quantum graph as described above supports topological resonances if and only if it contains a cycle.

This can be shown following similar ideas as in [20]. Let us first consider any scattering graph that does not contain a cycle. Such a graph is a tree (and to satisfy the requirement $d \geq 2$ all the canopy edges must be leads). The wave function for a bound state has to vanish on all the leads in order to be square-integrable. The remaining edges (bonds) form a finite tree whose leaves are at one end only connected to leads. The matching conditions then imply that the wave function also has to vanish on all the leaves. The process can now be iterated on the

remaining tree, showing that there are no non-vanishing square-integrable solutions on a scattering tree graph (of finite cardinality). As a result there cannot be any topological resonances on a scattering graph without cycles. Now let us assume that the scattering graph contains a cycle and let us show that there are choices for the bond lengths that lead to bound states which we call *topological bound states*. Topological resonances are the remnants of topological bound states when the latter get mixed with the continuum by a generic choice of bond lengths. The mechanism is related to a similar phenomenon for closed graphs where it explains the structure of *scars* [20]. Let \mathcal{C} be a cycle in the graph that consists of $C = |\mathcal{C}|$ bonds as shown on the left in Fig. 2. Our assumptions (no loops) imply $C \geq 2$. Now let us construct a bound state on \mathcal{C} . We require that the wave function vanishes exactly outside \mathcal{C} . By continuity all vertices on \mathcal{C} are then nodal points. The wave function for any $b \in \mathcal{C}$ then has to be of the form $\pm \sin(kx_b)$ and the matching conditions reduce to the statement that the wave function and its derivative have to be continuous along the cycle. This implies the following two diophantine conditions:

$$k\ell_b = n_b \times \pi \quad \text{with } n_b \in \mathbb{N} \text{ for all } b \in \mathcal{C} \quad (5)$$

$$\sum_{b \in \mathcal{C}} n_b = 2s \quad \text{for some } s \in \mathbb{N}. \quad (6)$$

The above conditions can be satisfied for a discrete sequence of wave numbers if and only if the bond lengths on \mathcal{C} are rationally dependent. This means that there exists a unit of length $\ell_0 > 0$ such that $\ell_b = i_b \ell_0$ for some $i_b \in \mathbb{N}$. One finds topological bound states on the cycle for wave numbers nk_0 ($2nk_0$) with $n \in \mathbb{N}$ if $\sum_{b \in \mathcal{C}} i_b$ is even (odd). The only reason for the existence of such states is the combination of a topological structure (the cycle) with destructive interference at the nodes.

A generic (rationally independent) choice of bond lengths will destroy topological bound states on the cycle as the conditions (5) and (6) cannot be satisfied exactly. However the condition can be satisfied approximately – to arbitrary precision at appropriate wave numbers. This is where the destroyed topological bound states leave a mark in the form of topological resonances.

Let us now show that topological resonances on cycles indeed lead to the statistical signatures that we observed in the numerical simulations reported above. For this we consider a connected scattering graph with girth $C \geq 2$ and focus our attention on the corresponding cycle. Each vertex has two attached bonds which belong to the cycle and at least one additional attached edge that does not belong to the cycle (as shown in the left part of Fig. 2). We will show that the ratio ρ of the intensity inside the cycle to the intensity outside has a distribution with a power-law tail $P(\rho) \sim \rho^{-\mu_C - 1}$ with $\mu_C = \frac{C+1}{2}$. For simplicity we will assume that all vertices on \mathcal{C} have the same degree $d = 3$ (the calculation for the general case follows the same steps but is too cumbersome for this note). Since we only want to compare the intensity

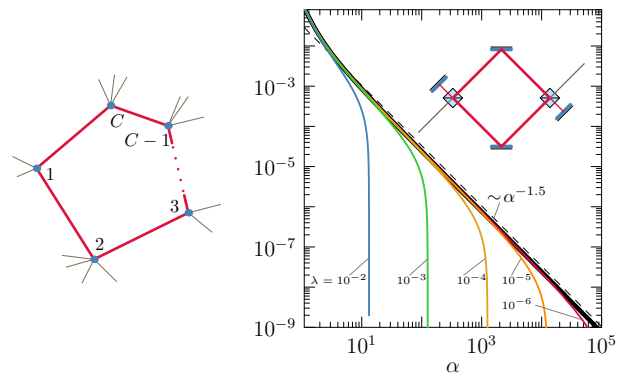


FIG. 2. (Color online) Left: A cycle of length C . Right: Numerically obtained tail of the integrated distribution $I(\alpha)$ of the mean intensity for a lossy beam-splitter setup (see inset).

inside the cycle to the intensity on the edges that are adjacent to the vertices on the cycle we may disregard the rest of the graph and replace the adjacent edges by leads of infinite length. We have thus reduced the problem to finding the scattering solutions for one cycle of length C with one lead at each vertex. The mean intensity on the cycle is defined as in (4) where the sum is restricted to bonds on \mathcal{C} . Combining the amplitudes in one vector $\mathbf{a}_{\mathcal{C}}$ one finds (see [14, 15])

$$\mathbf{a}_{\mathcal{C}} = \left(\mathbb{1} - e^{ik\ell/2} \sigma_{\mathcal{C}\mathcal{C}} e^{ik\ell/2} \right)^{-1} e^{ik\ell/2} \sigma_{\mathcal{C}\mathcal{L}} \mathbf{b}_{\mathcal{L}}^{\text{in}} \quad (7)$$

Here ℓ is a diagonal matrix of size $2C \times 2C$ that contains each bond length of the cycle twice, $\mathbf{b}_{\mathcal{L}}^{\text{in}}$ are amplitudes of incoming waves on the leads such that the mean intensity outside the cycle is proportional to $|\mathbf{b}_{\mathcal{L}}^{\text{in}}|^2$ (flux conservation ensures that the outgoing waves have the same intensity). The $2C \times 2C$ matrix $\sigma_{\mathcal{C}\mathcal{C}}$ and the $2C \times C$ matrix $\sigma_{\mathcal{C}\mathcal{L}}$ contain scattering amplitudes that can be derived from the Neumann matching conditions at the vertices. They are given by

$$\sigma_{\mathcal{C}\mathcal{L}} = \frac{2}{3} \begin{pmatrix} P \\ \mathbb{1} \end{pmatrix}; \quad \sigma_{\mathcal{C}\mathcal{C}} = \frac{1}{3} \begin{pmatrix} 2P & -\mathbb{1} \\ -\mathbb{1} & 2P^T \end{pmatrix} \quad (8)$$

where P is the permutation matrix for the cyclic permutation $(12 \dots C)$. The sub-unitary matrix $\sigma_{\mathcal{C}\mathcal{C}}$ has one eigenvalue equal to one with the eigenvector $\mathbf{v}_0 = \begin{pmatrix} \mathbf{1}_C^T \\ -\mathbf{1}_C^T \end{pmatrix}^T$ where $\mathbf{1}_C$ is the C -dimensional vector with unit entries. Bound states appear whenever

$$\Sigma(k) = e^{ik\ell/2} \sigma_{\mathcal{C}\mathcal{C}} e^{ik\ell/2} \quad (9)$$

has an eigenvalue equal to one. This happens if $e^{ik\ell/2} = \mathbb{1}$ which cannot be satisfied for generic (rationally independent) bond lengths and $k > 0$. However, in that case $k \mapsto e^{ik\ell/2}$ is an ergodic flow on a C -torus and $e^{ik\ell/2} = \mathbb{1}$ defines a point on the torus that can be approached to arbitrary precision as k increases [21]. Defining the ratio of intensities as $\rho(k) = |\mathbf{a}_{\mathcal{C}}|^2 / |\mathbf{b}_{\mathcal{L}}^{\text{in}}|^2$ we

may derive a power law tail for $P(\rho) = \langle \delta(\rho - \rho(k)) \rangle_k$ by replacing the spectral average by a torus average $P(\rho) = (2\pi)^{-C} \int d^C \boldsymbol{\theta} \delta(\alpha - \alpha(\boldsymbol{\theta}))$ where we have replaced the $2C \times 2C$ -matrix $e^{ik\ell}$ by a diagonal matrix $e^{i\boldsymbol{\theta}}$ that parameterizes the C -torus (each angle θ_j appears twice). Focussing on the contribution from a small region around $\boldsymbol{\theta} = \mathbf{0}$ where $\Sigma(\boldsymbol{\theta})$ has an eigenvalue one which dominates the behaviour. Second-order perturbation then yields

$$\rho(\boldsymbol{\theta}) \sim \frac{f^{(2)}(\hat{\boldsymbol{\theta}})}{\bar{\theta}^2 + [g^{(2)}(\hat{\boldsymbol{\theta}})]^2} \quad (10)$$

where $\bar{\theta} = \frac{1}{C} \sum_{n=1}^C \theta_n$ and $\hat{\theta}_n = \theta_n - \bar{\theta}$. The functions $f^{(2)}(\hat{\boldsymbol{\theta}})$ and $g^{(2)}(\hat{\boldsymbol{\theta}})$ are (explicitly known [22]) positive definite quadratic forms in the variables $\hat{\theta}_n$. This implies $P(\rho) \sim \rho^{-\mu_C-1}$ with $\mu_C = \frac{C+1}{2}$.

Coming back to the full graph that contains C as a subgraph, note that the mean intensity α on the graph contains a contribution proportional to ρ from the cycle. As a consequence the tail of $P(\alpha)$ cannot decay faster than the tail of $P(\rho)$ such that μ_C gives a lower bound for the exponent μ . This is consistent with our numerical findings (2) if $L \geq C - 1$. The exponent $\mu = \frac{L+2}{2}$ for $L < C - 1$ is consistent with the random-matrix approach and can be derived as a lower bound for the exponent in the present context following similar ideas [6–8]. Note however that our simulations were performed on regular structures where the connectivity does not vary strongly and where at most one lead was connected to one vertex. If we want (2) to be true in other circumstances we need to redefine L appropriately. E.g. one may show that if there are many leads at the same vertex with Neumann matching conditions there is still only one open quantum channel that couples to the inside of the graph. Moreover if a graph has a (possibly large) subgraph that is weakly connected to the rest (e.g. via a single bridge) then there is only a small number of channels which connect to the subgraph. The following definition will take care of these issues. Consider a connected subgraph H . A vertex v is on the boundary ∂H of that subgraph if it is adjacent to at least one edge in H and at least one edge outside H . We redefine L as the minimum of the size (cardinality) of ∂H over all connected subgraphs H that contain a cycle and that contain no lead. This reduces to the number of attached leads for the numerical simulations presented before. With this definition we conjecture that the result (2) we have found remains true for generic scattering graphs with Neumann matching conditions. We have excluded loops as they always lead to topological bound states that cannot be destroyed by changing the length of the loop. One may allow loops if one defines C as the shortest cycle which is not a loop. Dangling bonds have been excluded because they lead to a further set of topological resonances on paths between two vertices

with degree one (i.e. between two vertices with mirror-like reflection) – (2) will remain correct if C is redefined appropriately [22]. Let us also mention that measuring the intensity on one point of the graph will in general give a different but predictable power-law exponent – they are related to the local topological structure (e.g. the smallest cycle that contains the point) rather than the global topology. Only very regular graphs like the ones we used in Fig. 1 have the same power-law exponent at every point in the graph (and thus also for the mean intensity). However, other global quantities which are used to characterize resonances, such as e.g., the Wigner delay time or the resonance widths can be shown to distribute as the parameter α which was used here to render the theoretical discussion more transparent.

The derivation of the exponents (2) made explicit use of some properties of the Neumann matching conditions. The derivation can be generalised to other continuous matching conditions. For non-continuous matching conditions topological resonances as defined above can be constructed but more complex topological features are reflected in the exponents of the corresponding power laws. In Fig. 2 (right panel) we give numerical evidence of a topological resonance in a graph structure with matching conditions that can be realized in a laser experiment using beam-splitters and mirrors. The numerics show a clear power-law distribution with exponent $\mu = 3/2$ (dashed line). We have also included loss (e.g. at the reflection from mirrors) – we characterize the loss by the parameter λ which gives the fraction of photons which are lost when travelling once through the whole system. Lossy setups follow the power-law behaviour up to a cut-off that increases as losses decrease. Reducing losses to $\lambda = 10^{-5}$ may be within reach [23] showing that topological resonances may be observed in experiment.

The narrow resonances in networks play a very significant role in the presence of a nonlinearity as present in nonlinear optical wave guides or active optical fibres. The enhanced intensity at a topological resonance amplifies the nonlinearity to such an extent that the perturbative treatment breaks down and typical nonlinear effect such as hysteresis appear [24]. A detailed discussion and classification of topological resonances is now in preparation [22].

ACKNOWLEDGMENTS

SG and HS thank the Weizmann Institute of Science for hospitality. This work has been supported the EPSRC research network ‘Analysis on Graphs’ (EP/I038217/1). We would like to thank Nir Davidson, Micha Nixon, Daniel Waltner, and Jens Bolte for fruitful discussion.

-
- [1] B. Huckestein, R. Ketzmerick, C.H. Lewenkopf, Phys. Rev. Lett., **84**, 5504 (2000).
- [2] M.Mendoza, P.A. Schulz, R.O. Vallejos, C.H. Lewenkopf Phys. Rev. B **77**, 155307 (2008).
- [3] J.P. Bird, R. Akis, D.K. Ferry, Phys. Scr. **T90**, 50 (2001)
- [4] C. Texier, A. Comtet, Phys. Rev. Lett. **82**, 4220 (1999).
- [5] Y.V. Fyodorov, JETP Letters **78**, 250 (2003).
- [6] C.H. Lewenkopf, H.A. Weidenmüller, Ann. Phys. **212**, 53 (1991).
- [7] Y.V. Fyodorov, H.J. Sommers, J. Math. Phys. **38**, 1918 (1997).
- [8] H.J. Sommers, Y.V. Fyodorov, M. Titov, J. Phys. A **32**, L77 (1999).
- [9] R. Blümel, U. Smilansky, Phys. Rev. Lett. **64**, 241 (1990).
- [10] P. Gaspard and S. Rice, J. Chem. Phys. **90** 2225 (1989); J. Chem. Phys. **90** 2242 (1989); J. Chem. Phys. **90**, 2255 (1989).
- [11] M. Novaes, Phys. Rev E **85** 036202 (2012).
- [12] T. Kottos and U. Smilansky, Phys. Rev. Lett. **79**,4794-4797, (1997)
- [13] Sven Gnutzmann and Uzy Smilansky, Advances in Physics bf 55 (2006) 527-625.
- [14] T. Kottos, U. Smilansky, Phys. Rev. Lett. **85**, 968 (2000).
- [15] T. Kottos and U. Smilansky, J. Phys. A **36**, 3501 (2003).
- [16] V. Kostykin, R. Schrader, J. Phys. A **32**, 595 (1999).
- [17] P. Kuchment, J. Phys. A **38**, 4887 (2005).
- [18] B.S. Ong, *Spectral problems of optical waveguides and quantum graphs*, PhD thesis (Texas A& M University, 2006).
- [19] E.B. Davies, A. Pushnitski, Analysis & PDE, **4**, 729 (2011).
- [20] H. Schanz, T. Kottos, Phys. Rev. Lett. **90**, 234101 (2003).
- [21] F. Barra, P. Gaspard, J. Stat. Phys. **101**, 283 (2000).
- [22] S. Gnutzmann, H. Schanz, U. Smilansky, in preparation.
- [23] N. Davidson, M. Nixon, private communication.
- [24] S. Gnutzmann, U. Smilansky, S. Derevyanko, Phys. Rev. A **83**, 033831 (2011).